

Tritium beta decay with modified neutrino dispersion relations: KATRIN in the dark sea

Guo-yuan Huang^{1,*} and Werner Rodejohann^{1,†}

¹*Max-Planck-Institut für Kernphysik, Saupfercheckweg 1, 69117 Heidelberg, Germany*

We discuss beta decays in a dark background field, which could be formed by dark matter, dark energy or a fifth force potential. In such scenarios, the neutrino's dispersion relation will be modified by its collective interaction with the dark field, which can have observable consequences in experiments using tritium beta decays to determine the absolute neutrino mass. Among the most general interaction forms, the (pseudo)scalar and (axial-)vector ones are found to have interesting effects on the spectrum of beta decays. In particular, the vector and axial-vector potentials can induce distinct signatures by shifting the overall electron energy scale, possibly beyond the usually defined endpoint. The scalar and pseudoscalar potentials are able to mimic a neutrino mass beyond the cosmological bounds. We have placed stringent constraints on the dark potentials based on the available experimental data of KATRIN, and the sensitivity of future KATRIN runs is also discussed.

I. INTRODUCTION

The Mikheyev-Smirnov-Wolfenstein (MSW) effect of neutrino oscillations has been well established and understood [1–15]. The weak interactions between neutrinos and other fermions (e , p and n) lead to a modified dispersion relation when neutrinos traverse matter. Besides this established phenomenon, there might be three interesting scenarios in which neutrinos feel a background of particles in the “dark sea”. In such scenarios, neutrino kinematics is expected to be collectively altered by

- a background of ultralight dark matter, dark radiation or dark energy coupled to neutrinos. The ultralight field can be treated as a classical one, and the neutrino dispersion relation is affected simply by assigning an expectation value to the dark field in the Lagrangian. Modified neutrino oscillations in such scenarios have been discussed in detail in the literature [16–33];
- coherent forward scattering of neutrinos with light dark matter particles, which could be scalar or vector, the so-called “dark

NSI” [34]. In this case, it is the elastic scattering of the neutrino wave function off the dark matter grid which changes the dispersion relation. The form of the dark potential depends on the type of interaction between dark matter χ and neutrinos. If χ is a scalar particle, the process $\nu + \chi \rightarrow \nu + \chi$ can give rise to a correction to the neutrino mass [34];

- a fifth force sourced by heavy dark matter [35] or by ordinary matter [36–45]. This can be regarded as a special case of coherent forward scattering, as the mass of the scattering mediator is extremely small, such that the interaction is described by a long-range force. The fifth force as a classical virtual field is able to directly modify the neutrino propagation, similar to the motion of electrons in a Coulomb potential.

An immediate question arises: will these modified dispersion relations affect β -decay neutrino mass searches in which kinematics is used to determine m_ν ? If yes, how? We will provide here a systematic analysis with emphasis on the ongoing KATRIN experiment [46–48], which has recently set the world-leading model-independent constraint on the absolute neutrino mass.

Despite various realizations of the dark po-

* guoyuan.huang@mpi-hd.mpg.de

† werner.rodejohann@mpi-hd.mpg.de

tential, our results will be presented in a form as model-independent as possible, such that they can be applied to various scenarios.

II. DARK MSW EFFECT

Regardless of the nature of the underlying interaction, the neutrino will feel a “dark potential” that can only have five different forms [49, 50]:

$$-\mathcal{L} \supset (g_\phi \phi \bar{\nu} \nu + g_\varphi \varphi \bar{\nu} \gamma_5 \nu + g_V V_\mu \bar{\nu} \gamma^\mu \nu + g_a a_\mu \bar{\nu} \gamma_5 \gamma^\mu \nu + g_T T_{\mu\nu} \bar{\nu} \sigma^{\mu\nu} \nu) \delta_M. \quad (1)$$

Here $\delta_M = 1/2$ (1) if neutrinos are Majorana (Dirac) particles, and $\phi, \varphi, V_\mu, a_\mu$ and $T_{\mu\nu}$ represent real scalar, pseudoscalar, vector, axial-vector and tensor fields, respectively. The neutrino field is composed of $\nu = \nu_L + \nu_L^c$ for Majorana neutrinos, and $\nu = \nu_L + \nu_R$ for Dirac neutrinos. For Dirac neutrinos, the coupling constants g_ϕ, g_V and g_a are Hermitian matrices in general, while g_φ is anti-Hermitian. For the Majorana case, g_ϕ and g_a are real symmetric matrices, while g_φ and g_V are purely imaginary symmetric and antisymmetric matrices, respectively.

The fields $\phi, \varphi, V_\mu, a_\mu$ and $T_{\mu\nu}$ do not necessarily correspond to real particles, e.g., they may represent contributions from coherent forward scattering or virtual fifth forces. Note that here we assume the field $X = \phi, \varphi, V_\mu, a_\mu, T_{\mu\nu}$ to be real, and only the overall sign combined with “charge” $g_X X$ matters for neutrinos.

A well-known example is already given by the standard MSW effect. For instance, via the charged-current interaction with electrons in the Earth, the neutrino will feel a tiny potential of the form $g_V V_0 + g_a a_0 = \sqrt{2} G_F n_e$, where G_F is the

Fermi constant, n_e is the electron number density, and the isotropic spatial components $g_a a$ are averaged out.

Our results are simplified by imposing the assumption that the dark field is purely time-like, i.e., we assume from the cosmological principle that the preference of spatial orientation of the background is not significant or simply averaged out. Hence, the antisymmetric tensor field $T_{\mu\nu}$ [20] is vanishing in our context.

The equation of motion (EOM) of the neutrino wave function given the interactions in Eq. (1) is described by

$$\left[\gamma^\mu (i\partial_\mu - g_V V_\mu + g_a a_\mu \gamma_5) - (\widehat{M}_\nu + g_\phi \phi + g_\varphi \varphi \gamma_5) \right] \nu = 0, \quad (2)$$

where the neutrino is written in the mass eigenstate basis in vacuum, therefore the mass matrix \widehat{M}_ν is diagonal. We can assume that three generations of neutrinos share the same coupling, i.e., $g_X \propto 1$ for all coupling constants, which in particular implies that there is no effect in neutrino oscillations. Note that for Majorana neutrinos, the diagonal vector interactions will be vanishing.

The collective effect of the dark sea is to modify the dispersion relation of neutrinos, which can be obtained by multiplying $\gamma^\mu (i\partial_\mu - g_V V_\mu + g_a a_\mu \gamma_5) + (\widehat{M}_\nu + g_\phi \phi - g_\varphi \varphi \gamma_5)$ to the left of Eq. (2). For the plane-wave solution we have $i\partial_\mu \nu = p_\mu \nu$, such that $\nu \propto \exp(-i E_\nu \cdot t + i \mathbf{p}_\nu \cdot \mathbf{x})$, where E_ν is yet to be fixed. Ignoring the cross terms of the background fields (i.e., we turn on only one field at a time), we end up with the following dispersion relation for neutrinos:

$$(E_\nu - g_V V_0)^2 = (|\mathbf{p}_\nu| - \hat{\mathbf{p}} \cdot \boldsymbol{\Sigma} g_a a_0)^2 + (\widehat{M}_\nu + g_\phi \phi)^2 + (|g_\varphi| \varphi)^2, \quad (3)$$

where E_ν and \mathbf{p}_ν are the energy and momentum of the neutrino, $\hat{\mathbf{p}}$ denotes the direction of the momentum, and $\boldsymbol{\Sigma} \equiv \gamma_5 \gamma_0 \boldsymbol{\gamma}$ stands for

the spin operator. Eq. (3) has typically two energy solutions: the upper one (positive for most cases) corresponds to the particle $\nu^{(+)}$, and

the lower one (mostly negative), which is not bounded from below, should be interpreted as the antiparticle $\nu^{(-)}$. For the antineutrino, the direction of the momentum $\hat{\mathbf{p}}$ should be reversed along with the energy accordingly.

Eq. (3) implies that the scalar and pseudoscalar potentials $g_\phi\phi$ and $|g_\varphi|\varphi$ simply add to the vacuum mass term. The vector potential $g_V V_0$ shifts the overall energy of neutrinos. The axial-vector potential $g_a a_0$ will lead to helicity-dependent energies of the states with $\hat{\mathbf{p}} \cdot \Sigma \nu^{(+)} = \pm \nu^{(+)}$ for neutrino and $-\hat{\mathbf{p}} \cdot \Sigma \nu^{(-)} = \pm \nu^{(-)}$ for antineutrino, where ‘ \pm ’ stands for the right- and left-helicity states, respectively. This split of energies is discussed in Appendix A. In the massless limit, i.e., $\widehat{M}_\nu = 0$, the difference between the vector and axial vector interactions vanishes for the active neutrino ν_L , because the left- and right-handed fields are decoupled. More details on the derivation of the dispersion relation and how the neutrino should be canonically quantized in the dark background are presented in Appendices A and B.

III. SIGNALS AT KATRIN

Neutrino oscillations in the dark potentials have been widely discussed in the literature [16–45]. However, the sensitivity of oscillation experiments is limited by the specific setup of the dark potential. For example, if three generations of neutrinos couple identically to the dark field, similar to the neutral Z -exchange in the Standard Model, the neutrino oscillation is blind to the potential no matter how the dark fields behave. Furthermore, if ultralight dark matter is responsible for the dark potential, and the dark field is fast oscillating over the baseline $\gtrsim \mathcal{O}(100 \text{ m})$ (the minimal baseline for which neutrino oscillations have been observed), neutrinos in flight will experience a vanishing averaged effect. Thus, the microscopic nature of the nuclear beta decay related to electron neutrinos makes it an excellent complementary probe of the dark potential.

In the absence of the dark field, the rate of

beta decays, ${}^3\text{H} \rightarrow {}^3\text{He} + e^- + \bar{\nu}_e$, reads [51–55]

$$\frac{d\Gamma_\beta}{dK_e} = N_T \frac{\bar{\sigma}(E_e)}{\pi^2} \sum_{i=1}^3 |U_{ei}|^2 H(E_e, m_i), \quad (4)$$

where N_T is the total target mass of ${}^3\text{H}$, and E_e is the electron energy. The reduced cross section is given as

$$\bar{\sigma}(E_e) \equiv \frac{G_F^2}{2\pi} |V_{ud}|^2 F(Z, E_e) (\bar{g}_V^2 + 3\bar{g}_A^2) \frac{m_{^3\text{He}}}{m_{^3\text{H}}} \times E_e \sqrt{E_e^2 - m_e^2}, \quad (5)$$

where $G_F = 1.166 \times 10^{-5} \text{ GeV}^{-2}$, $|V_{ud}| \approx \cos \theta_C$ with the Cabibbo angle $\theta_C \approx 12.8^\circ$, $F(Z, E_e) = 2\pi\eta/(1 - e^{-2\pi\eta})$ is the ordinary Fermi function due to the distortion of the electron in the nuclear Coulomb potential, $\eta \equiv Z\alpha E_e/p_e$ with p_e being the electron momentum and $\alpha \approx 1/137$, and $\bar{g}_V \approx 1$ and $\bar{g}_A \approx 1.247$ stand for the vector and axial-vector coupling constants of weak interactions of tritium, respectively. The kinematics of the beta-decay spectrum is contained in (defining $K_e = E_e - m_e$)

$$H(E_e, m_i) \approx \sqrt{(K_{\text{end},0} - K_e)^2 - m_i^2} \quad (6) \\ \times (K_{\text{end},0} - K_e),$$

where $K_{\text{end},0} = [(m_{^3\text{H}} - m_e)^2 - m_{^3\text{He}}^2]/(2m_{^3\text{H}})$ is the endpoint energy in the relativistic theory assuming a vanishing neutrino mass. The actual endpoint energy for the neutrino mass m_i is approximately given by

$$K_{\text{end}} = K_{\text{end},0} - m_i. \quad (7)$$

As mentioned above, the scalar and pseudoscalar potentials merely add an effective mass term to neutrinos, which is kinetically indistinguishable from the vacuum mass. In fact, in some scenarios they are even postulated to be the origin of small neutrino masses [35]. However, we need to emphasize that since the current dark potential is expected to be different from that in the early Universe, the model-dependent cosmological bounds on the absolute neutrino mass, e.g. $\Sigma < 0.12 \text{ eV}$ [56], can be evaded or weakened. This will possibly lead to

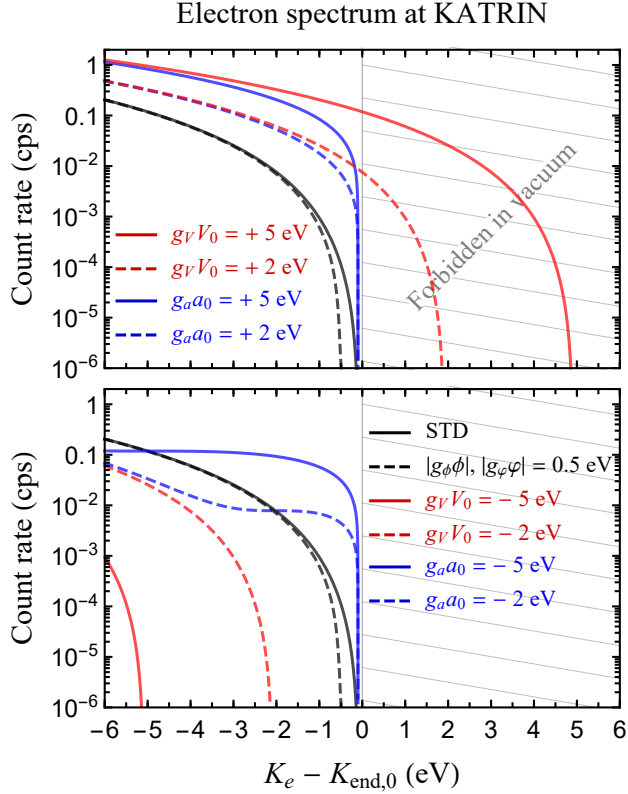


FIG. 1. The integrated beta-decay spectra at KATRIN in various types of dark seas: vector potentials with $g_V V_0 = \pm 5$ eV (solid red curves) and $g_V V_0 = \pm 2$ eV (dashed red curves) as well as axial-vector potentials with $g_a a_0 = \pm 5$ eV (solid blue curves) and $g_a a_0 = \pm 2$ eV (dashed blue curves). For these curves, the neutrino mass has been fixed to $m_1 = 0.1$ eV. Contributions from ϕ and φ which mimic a neutrino mass exceeding cosmological bounds are shown as the dashed black curve.

large signals in future KATRIN runs, which expect no visible effect of neutrino masses if the stringent cosmological bounds are adopted.

The vector potential has a profound effect on the beta-decay spectrum. To clearly see that, we pick out from Eq. (3) the vector contribution to the neutrino energy

$$E_\nu = \pm \sqrt{\mathbf{p}_\nu^2 + m_i^2} + g_V V_0 . \quad (8)$$

For the antineutrino mode, the resulting energy is not bounded from below, which should be reversed by redefining the creation and annihilation operators as in standard textbooks. This

gives $\bar{E}_\nu = \sqrt{\mathbf{p}_\nu^2 + m_i^2} - g_V V_0$ for the antiparticle, indicating that the neutrino and antineutrino excitations feel opposite vector potentials, which is to be expected. This implies that neutrino mass experiments using electron capture such as ECHo [57], will see an opposite effect compared to KATRIN, providing a way to independently test the effect¹.

An astonishing implication of Eq. (8) is that the antineutrino energy of beta decays in the vector background can run into the negative (but bounded), when $g_V V_0 > \sqrt{\mathbf{p}_\nu^2 + m_i^2}$. The beta-decay spectrum can hence extend beyond the normal kinematic limit $K_{\text{end},0}$. This is not a surprise as the process which is not kinematically allowed in vacuum can take place if the medium modifies the dispersion relations [9], a phenomenon familiar in, e.g., plasmon decay. As a consequence, the electron endpoint energy in Eq. (7) will be shifted towards

$$\begin{aligned} \tilde{K}_{\text{end}} &= \frac{(m_{^3\text{H}} - m_e + g_V V_0)^2 - (m_{^3\text{He}} + m_i)^2}{2(m_{^3\text{H}} + g_V V_0)} \\ &\approx K_{\text{end},0} - m_i + g_V V_0 . \end{aligned} \quad (9)$$

With a straightforward derivation, we find that the spectral function in the case of a dark vector field is well described by

$$\begin{aligned} \tilde{H}(E_e, m_i) &\approx \sqrt{(K_{\text{end},0} - K_e + g_V V_0)^2 - m_i^2} \\ &\times (K_{\text{end},0} - K_e + g_V V_0) , \end{aligned} \quad (10)$$

which should be compared to the vacuum case in Eq. (6), while the other terms in Eq. (4) remain unchanged.

Since the axial-vector interaction distinguishes two helicity states, in order to exactly calculate the spectrum we have to perform the integration over the unsummed helicity amplitudes. More detailed steps to obtain the spectrum with the modified neutrino dispersion relation are presented in Appendices A, B and C.

¹ We also note that if neutrinos are Majorana particles and lepton-number-violating interactions are present, an enhanced rate of $0\nu\beta\beta$ decay will also be expected.

In the relativistic limit (i.e., away from the endpoint), only the outgoing right-helicity antineutrino is active, and the vector and axial-vector cases should converge to each other. Note that also for the axial-vector case electron capture experiments will see an opposite effect compared to beta decay experiments.

In Fig. 1, we have illustrated the distortions of the beta-decay spectrum in various dark seas at KATRIN. The vector potential (red curves) shifts the whole spectrum to lower or higher endpoints, without changing the spectral shape. The kinematically forbidden region of the spectrum is reachable in the case of a dark vector potential, as we discussed previously. In comparison, the axial-vector potential (blue curves) induces a non-trivial distortion to the spectrum near the endpoint, but it indeed converges to the vector case away from the endpoint. The rapid rise of the event rate near the endpoint for the axial-vector case is due to a volume effect when we integrate over the phase space. At the minimum neutrino energy the neutrino phase space is non-vanishing in the presence of a_0 , in contrast to the vacuum case, see Appendix C. On the other hand, the scalar potentials ϕ and φ mimic the effect of the neutrino mass, shown as dashed black curves. They can induce an effective neutrino mass beyond the cosmological limit.

As long as the neutrino mass is not vanishingly small, the difference near the endpoint between the vector and axial-vector cases is as apparent as in Fig. 1. Only when the neutrino mass is comparable to time-scale of the background field formation (typically ~ 1 Gyr corresponding to 10^{-32} eV), the axial-vector scenario starts to approach the vector case. For further discussions, see Appendix D.

We continue with fitting KATRIN data to our scenarios. The effect of scalar and pseudoscalar potentials is identical to being from m_ν^2 . The consequences of vector and axial-vector potentials are the same at energies away from the endpoint, for which KATRIN collects the most events. Their major effect is to shift the overall energy scale of electrons, which can be rep-

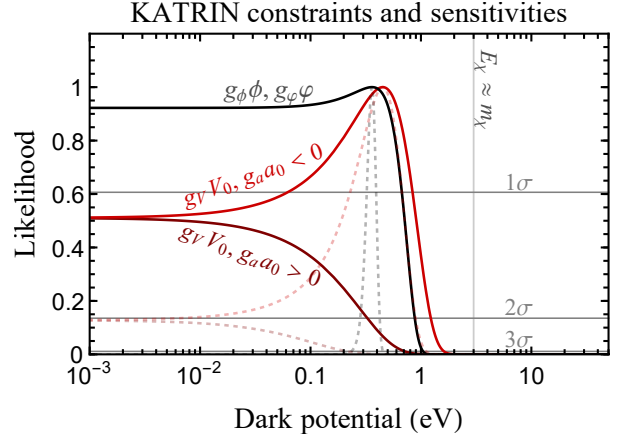


FIG. 2. The constraints on the dark potentials $g_V V_0$, $g_a a_0$, $g_\phi \phi$ and $g_\varphi \varphi$ using the data of KATRIN’s first and second campaigns, shown as the solid curves. The sensitivities corresponding to the ultimate KATRIN goal $m_\nu < 0.2$ eV at 90% level, i.e., $\sigma(m_\nu^2) = 0.025$ eV² [58], along with a reduced potential fluctuation by a factor of three are given as the dotted lighter curves. The horizontal gray lines represent $\Delta\chi^2 = 1, 4$ and 9 , respectively. The maximally allowed values of $g_0 V_0$ and $g_a a_0$ in the framework of a fifth force sourced by dark matter are shown as the vertical line.

resented by the endpoint energy, e.g., $E_0 \equiv K_{\text{end},0} + g_V V_0$ for vector, at vanishing neutrino masses in the KATRIN fits. The endpoint E_0 and the squared neutrino mass m_ν^2 are regarded as free parameters in the KATRIN fits [46–48]. We perform our own fit of available KATRIN KNM1 data [46], including however for simplicity only positive m_ν^2 for the vector and axial-vector cases. Marginalizing over m_ν^2 , our fit result on the endpoint will be compared with the expected value, and this is then used to set a limit on $g_V V_0$.

The fit yields $E_0 = 18573.79 \pm 0.04$ eV, and technical details can be found in Appendix E. The actual Q -value is obtained by correcting for molecular recoil (1.72 eV) and potential fluctuations of the tritium source and main spectrometer (-0.2 ± 0.5 eV for KNM1), which gives $Q = 18575.31 \pm 0.5$ eV, slightly smaller than the expectation of 18575.72 ± 0.07 eV. For the KNM2 data [48], we directly use the

official results $E_0 = 18573.69 \pm 0.03$ eV and $m_\nu^2 = 0.26 \pm 0.34$ eV² (which is mostly in the positive regime) to generate the χ^2 for our dark potentials. For the (pseudo)scalar potential, we assume the vacuum mass to be vanishing.

Combining KATRIN's two campaigns by adding the χ^2 , the likelihood $L = \exp(-\Delta\chi^2/2)$ for our dark potentials is given in Fig. 2. The 2σ limits corresponding to $\Delta\chi^2 < 4$ read $-1.3 \text{ eV} < (g_V V_0, g_a a_0) < 0.3 \text{ eV}$ and $(|g_\phi \phi|, |g_\varphi \varphi|) < 0.9 \text{ eV}$. The fact that the limits on $|g_\phi \phi|$ and $|g_\varphi \varphi|$ are quite close to the official KATRIN limits on neutrino mass, which as discussed above is indistinguishable from the (pseudo)scalar potential case, implies that our fitting procedure is correct and trustworthy. For potential values smaller than $\mathcal{O}(1)$ eV, the χ^2 is dominated by events away from the endpoint, where the effects of vector and axial-vector become almost the same. Note that because in KATRIN fits the endpoint energy E_0 is taken to be completely free without any priors, the vector and axial-vector potentials will not affect the current neutrino mass results.

A slight preference of the (axial-)vector potential $g_V V_0 = -0.45$ eV can be noted. The current sensitivity of KATRIN is not sufficient to distinguish the vector and axial-vector cases. Keeping the best-fit values so far, the future sensitivities to reach the reference KATRIN target $m_\nu < 0.2$ eV and by reducing potential fluctuations by a factor of three are shown as the dotted curves.

IV. A CONCRETE EXAMPLE

Even though we aim to present the results as model-independent as possible, it is worthwhile to remark on the phenomenology in a specific framework.

Suppose that there is a long-range force $g_\chi A'_\mu \bar{\chi} \gamma^\mu \chi + g_\nu A'_\mu \bar{\nu} \gamma^\mu \nu$ between ν (by mixing) and fermionic dark matter χ mediated by a neutrinoophilic dark vector A' [59] (similar considerations hold for a scalar). After integrating out the dark matter configurations, one ends up with an effective potential $g_\nu \langle A'_0 \rangle \bar{\nu} \gamma^0 \nu$ [42].

The resulting neutrino potential $|g_V V_0|$ is given by [35, 40]

$$\frac{g_\nu g_\chi n_\chi}{m_{A'}^2 + m_D^2} \approx 1.1 \text{ eV} \left(\frac{\rho_\chi}{0.3 \text{ GeV} \cdot \text{cm}^{-3}} \right) \times \left(\frac{7 \text{ keV}}{m_\chi} \right) \left(\frac{0.01 g_\chi}{g_\nu} \right) \frac{(1.95 \text{ K})^2}{T_\nu^2 + m_{A'}^2/g_\nu^2}, \quad (11)$$

where $m_{A'}$ is the mass of the dark vector which could be generated via the Stückelberg mechanism [60], ρ_χ is the local dark matter density and $m_D \sim g_\nu T_\nu$ is a screening scale set by the Debye length with T_ν being the temperature of ambient neutrinos. The long-range force parameters can be set to be very small, e.g., $m_{A'} = 10^{-21}$ eV and $g_\nu = 10^{-17}$, such that no laboratory bounds² other than beta decays can apply to the concerned parameter space.

One might be concerned about astrophysical limits from the likes of BBN, CMB, LSS and supernovae, where the dark matter or neutrino density is much higher than in the Earth. However, various arguments attempting to constrain this type of force are mostly invalid due to the screening effect in the dense environment; for relevant details see Refs. [35, 62]. The strongest bounds we can find, $g_\nu \lesssim 10^{-7}$ from CMB free streaming [35], $g_\chi \lesssim 4 \times 10^{-3} (m_\chi/\text{GeV})^{3/4}$ from dark matter collision [63–65] and $m_{A'} \gtrsim 10^{-27}$ eV from tidal stream bounds [66–68], set basically no meaningful limit on the dark potential, i.e., $|g_V V_0| \lesssim 10$ TeV. The dark matter dispersion relation will also be affected in the halo. To be consistent with the given ρ_χ , we require the dark matter self-potential to be smaller than $m_\chi/10$, which imposes $|g_V V_0| < 3$ eV in Fig. 2. Hence, probing this type of model via neutrino kinematics in beta decays turns out to be the most sensitive approach.

V. OUTLOOK

We have performed a systematic study on the effects of dark neutrino potentials on beta-decay,

² If the new force also couples to charged particles, e.g., electrons, there will be strong constraints from tests of the equivalence principle [61].

especially focusing on the ongoing KATRIN experiment. By collectively interacting with background fields, neutrinos will have dispersion relations different from the ones in vacuum, which induces distinct distortions to the beta-decay spectrum. Observable consequences include neutrino mass signals beyond the ones bounded from cosmological constraints, events beyond the kinematical endpoint of the decay, and spectral distortions. Limits were obtained using KATRIN data, which are stronger than all other limits in simple scenarios.

ACKNOWLEDGMENTS

The authors would like to thank Shu-Yuan Guo, Leonard Köllenberger, Newton Nath, Kathrin Valerius and Shun Zhou for valuable communications. This work is supported by the Alexander von Humboldt Foundation.

Appendix A: Massive neutrinos in an axial-vector background

The plane-wave solutions to the Dirac equations in the axial-vector background differ from the vacuum ones. To see that, we collect the left- and right-handed fields into $\nu = \nu_L + \nu_R$ ($\nu_R = \nu_L^c$ for Majorana neutrinos), which satisfies the equation of motion

$$(i\partial + g_a a_0 \gamma^0 \gamma^5 - m)\nu = 0. \quad (\text{A1})$$

For the positive and negative frequency modes, we have

$$(p_\mu \gamma^\mu + g_a a_0 \gamma^0 \gamma^5 - m)u(p, s) = 0, \quad (\text{A2})$$

$$(-p_\mu \gamma^\mu + g_a a_0 \gamma^0 \gamma^5 - m)v(p, s) = 0. \quad (\text{A3})$$

First of all, the energy eigenvalues should be derived. This can be done by multiplying a matrix $(p_\mu \gamma^\mu + g_a a_0 \gamma^0 \gamma^5 + m)$ from the left to Eq. (A2), yielding

$$[p^2 - (g_a a_0)^2 + 2g_a a_0 \mathbf{p} \cdot \boldsymbol{\Sigma} - m^2] u(p, s) = 0,$$

where $\boldsymbol{\Sigma} = \gamma^5 \gamma^0 \boldsymbol{\gamma}$ is simply the spin operator, and $\hat{\mathbf{p}} \cdot \boldsymbol{\Sigma}/2$ represents the helicity with eigenvalue $s = \pm 1/2$. Different from the vacuum

case, the neutrino energy is split for the two helicities by the temporal component of the background. The energy eigenvalues for both neutrino and antineutrino (the same for Majorana case) read

$$E_s = \sqrt{(|\mathbf{p}| - 2s \cdot g_a a_0)^2 + m^2}. \quad (\text{A4})$$

Note that the above equation does not apply to the massless case with $m = 0$ eV. By imposing the orthogonality conditions³,

$$\begin{aligned} u^\dagger(\mathbf{p}, s') u(\mathbf{p}, s) &= v^\dagger(\mathbf{p}, s') v(\mathbf{p}, s) = 2E_s \delta_{s's}, \\ u^\dagger(-\mathbf{p}, s') v(\mathbf{p}, s) &= v^\dagger(-\mathbf{p}, s') u(\mathbf{p}, s) = 0, \end{aligned} \quad (\text{A5})$$

the structure of the spinors u and v is found to be of the form

$$\begin{aligned} u(p, s) &= \frac{\not{p}_s + g_a a_0 \gamma^0 \gamma^5 + m}{\sqrt{(E_s + E_0)^2 - 4(s p - g_a a_0)^2}} u(0, s), \\ v(p, s) &= \frac{-\not{p}_s + g_a a_0 \gamma^0 \gamma^5 + m}{\sqrt{(E_s + E_0)^2 - 4(s p - g_a a_0)^2}} v(0, s), \end{aligned}$$

where $E_0 = \sqrt{(g_a a_0)^2 + m^2}$ is the neutrino energy at rest. Notice that for the spinor v , we have the relation $\hat{\mathbf{p}} \cdot \boldsymbol{\Sigma} v(p, s) = -2s v(p, s)$, in comparison to $\hat{\mathbf{p}} \cdot \boldsymbol{\Sigma} u(p, s) = 2s u(p, s)$. The helicity completeness relations of the spinors are

$$\begin{aligned} u(\mathbf{p}, s) \bar{u}(\mathbf{p}, s) &= (\not{p}_s + g_a a_0 \gamma^0 \gamma^5 + m) \\ &\quad \times \frac{1 + 2s \hat{\mathbf{p}} \cdot \boldsymbol{\Sigma}}{2}, \\ v(\mathbf{p}, s) \bar{v}(\mathbf{p}, s) &= (\not{p}_s - g_a a_0 \gamma^0 \gamma^5 - m) \\ &\quad \times \frac{1 - 2s \hat{\mathbf{p}} \cdot \boldsymbol{\Sigma}}{2}. \end{aligned} \quad (\text{A6})$$

It is easy to verify these relations with the help of the orthogonality conditions, and one recovers the standard results in the limit of $a_0 = 0$.

Expanding the field operator as $\nu = \int d^3 \mathbf{p} (b \nu_{p,s}^{(+)} + d^\dagger \nu_{p,s}^{(-)})$, we arrive at

$$\begin{aligned} \nu(x) = \sum_s \int \frac{d^3 \mathbf{p}}{(2\pi)^{3/2}} \sqrt{\frac{1}{2E_s}} &[b_{p,s} u(\mathbf{p}, s) e^{-ip_s \cdot x} \\ &+ d_{p,s}^\dagger v(\mathbf{p}, s) e^{ip_s \cdot x}], \end{aligned} \quad (\text{A7})$$

³ One can check that these orthogonality conditions guarantee the plane wave to be normalized under the field expansion Eq. (A7), e.g., $\int d^3 x \nu_{p',s'}^\dagger \nu_{p,s} = \delta^3(p' - p) \delta_{s's'}$.

where $b_{p,s}$ and $d_{p,s}^\dagger$ should be interpreted as the particle annihilation and antiparticle creation operators, respectively, for Dirac neutrinos. For Majorana neutrinos, the condition $\nu = \nu^c$ will force $b_{p,s} = d_{p,s}$, i.e., $b_{p,s}$ annihilates simultaneously the positive- and negative-frequency excitations. Using the orthogonality conditions, the canonical quantization rules of $\nu(x)$ consistently lead to

$$\begin{aligned} \{b_{p',s'}, b_{p,s}^\dagger\} &= \delta^3(\mathbf{p}' - \mathbf{p})\delta_{s's}, \\ \{d_{p',s'}, d_{p,s}^\dagger\} &= \delta^3(\mathbf{p}' - \mathbf{p})\delta_{s's}. \end{aligned} \quad (\text{A8})$$

The neutrino Hamiltonian with normal ordering can then be expanded as (e.g., for the Dirac case)

$$\mathcal{H} = \int d^3p \sum_s E_s (b_{p,s}^\dagger b_{p,s} + d_{p,s}^\dagger d_{p,s}). \quad (\text{A9})$$

Appendix B: Dirac neutrinos in a vector background

The results for the vector background are more straightforward. Given the EOM

$$(i\partial^\mu - g_V V^\mu - m)\nu = 0, \quad (\text{B1})$$

the plane-wave spinor should satisfy

$$[(p_\mu - g_V V_\mu)\gamma^\mu - m] u(p, s) = 0, \quad (\text{B2})$$

$$[(-p_\mu - g_V V_\mu)\gamma^\mu - m] v(p, s) = 0. \quad (\text{B3})$$

This leads to the energy eigenvalues

$$E_\pm = \sqrt{(\mathbf{p} \mp g_V \mathbf{V})^2 + m^2} \pm g_V V_0, \quad (\text{B4})$$

where “ \pm ” in E_\pm corresponds to the neutrino (u) and the antineutrino (v), respectively. Note again that these results do not apply to Majorana neutrinos. Hence, in principle one can distinguish Majorana and Dirac neutrinos by the experimental signature of the vector potential, if one would know that the interaction is diagonal in flavor.

The orthogonality conditions as well as the completeness relations are consistently given by

$$\begin{aligned} u^\dagger(\mathbf{p}, s') u(\mathbf{p}, s) &= v^\dagger(\mathbf{p}, s') v(\mathbf{p}, s) = 2\tilde{E}\delta_{s's}, \\ u^\dagger(-\mathbf{p}, s') v(\mathbf{p}, s) &= v^\dagger(-\mathbf{p}, s') u(\mathbf{p}, s) = 0, \end{aligned} \quad (\text{B5})$$

$$\begin{aligned} u(\mathbf{p}, s) \bar{u}(\mathbf{p}, s) &= (\tilde{p} + m) \frac{1 + 2s\hat{\mathbf{p}} \cdot \Sigma}{2}, \\ v(\mathbf{p}, s) \bar{v}(\mathbf{p}, s) &= (\tilde{p} - m) \frac{1 - 2s\hat{\mathbf{p}} \cdot \Sigma}{2}, \end{aligned} \quad (\text{B6})$$

where the effect of the dark background is absorbed into $\tilde{E} \equiv \sqrt{\tilde{\mathbf{p}}^2 + m^2} = E_\pm \mp g_V V_0$ with $\tilde{\mathbf{p}} = \mathbf{p} \mp g_V \mathbf{V}$, such that $\tilde{E}^2 - \tilde{\mathbf{p}}^2 = m^2$. Here, it is equivalent to replace $\hat{\mathbf{p}} \cdot \Sigma$ with $\gamma_5 \not{s}$, where $\not{s} \equiv (|\mathbf{p}|/m, \tilde{E}\hat{\mathbf{p}}/m)$. These relations should be used along with the expansion

$$\begin{aligned} \nu(x) = \sum_s \int \frac{d^3p}{(2\pi)^{3/2}} \sqrt{\frac{1}{2\tilde{E}}} &[b_{p,s} u(\mathbf{p}, s) e^{-ip_+ \cdot x} \\ &+ d_{p,s}^\dagger v(\mathbf{p}, s) e^{ip_- \cdot x}], \end{aligned} \quad (\text{B7})$$

or equivalently the form

$$\begin{aligned} \nu(x) = \sum_s \int \frac{d^3\tilde{\mathbf{p}}}{(2\pi)^{3/2}} \sqrt{\frac{1}{2\tilde{E}}} &[b_{p,s} u(\mathbf{p}, s) e^{-i\tilde{p} \cdot x} \\ &+ d_{p,s}^\dagger v(\mathbf{p}, s) e^{i\tilde{p} \cdot x}] e^{-ig_V V \cdot x}. \end{aligned} \quad (\text{B8})$$

Eqs. (B5), (B6) and (B8) indicate that one may think of all the relations with $\tilde{p} = \{\tilde{E}, \tilde{\mathbf{p}}\}$ similar as those in the vacuum. The net impact of the dark background is adding an overall phase $\exp(-ig_V V_0 t + ig_V \mathbf{V} \cdot \mathbf{x})$ to the neutrino field. Since other fields (e.g., n, p and e) do not feel this phase, it will enter into the factor $\delta^4(\cdots \pm g_V V)$ which imposes energy momentum conservation.

Ultimately, the Hamiltonian of neutrino field is found to be

$$\mathcal{H} = \int d^3p \sum_s (E_+ b_{p,s}^\dagger b_{p,s} + E_- d_{p,s}^\dagger d_{p,s}). \quad (\text{B9})$$

Appendix C: The beta-decay rate in the dark sea

The amplitude for the transition of beta decays is given by

$$\mathcal{M} = \frac{G_F V_{ud}}{\sqrt{2}} \bar{u}(p_e) \gamma^\mu (1 - \gamma_5) v(p_\nu) \times \bar{u}(p') \gamma_\mu (\bar{g}_V - \bar{g}_A \gamma_5) v(p), \quad (C1)$$

where the higher order magnetic and pseudoscalar form factors of the nucleons are neglected, and p, p', p_e and p_ν are the momenta of tritium, helium, electron and neutrino, respectively. Summing over the spins of particles other than neutrino, we arrive at

$$\sum_{s,s',s_e} |\mathcal{M}|^2 = \frac{G_F^2 |V_{ud}|^2}{2} \text{Tr} \left[(\not{p}_e + m_e) \gamma^\mu (1 - \gamma_5) v(p_\nu, s_\nu) \bar{v}(p_\nu, s_\nu) \gamma^\nu (1 - \gamma_5) \right] \times \text{Tr} \left[(\not{p}' + M') \gamma_\mu (\bar{g}_V - \bar{g}_A \gamma_5) (\not{p} + M) \gamma_\nu (\bar{g}_V - \bar{g}_A \gamma_5) \right], \quad (C2)$$

where for the unsummed spin bilinear of neutrinos $v(p_\nu, s_\nu) \bar{v}(p_\nu, s_\nu)$ under the impact of dark potentials, Eqs. (A6) and (B6) should be taken.

For the vector dark background, we are ready to sum over the final neutrino spin, i.e. $\sum v(\mathbf{p}, s) \bar{v}(\mathbf{p}, s) = \not{p} - m$. But for the axial-vector case, due to the split of energy levels discussed in Appendix A, the integration over phase space for two helicity states should be performed separately. This introduces extra complexity.

After the index contraction, the matrix element for the outgoing neutrino with $p_{\nu,s}$ in the

axial-vector background is

$$\begin{aligned} \sum_{s,s',s_e} |\mathcal{M}_a|^2 \approx & 16 G_F^2 |V_{ud}|^2 \left\{ (\bar{g}_V + \bar{g}_A)^2 (p_e \cdot p') \right. \\ & \times (p \cdot p_{\nu,s}) + (\bar{g}_V - \bar{g}_A)^2 (p_e \cdot p)(p' \cdot p_{\nu,s}) \\ & + (\bar{g}_A^2 - \bar{g}_V^2) M \cdot M' (p_e \cdot p_{\nu,s}) \\ & + 2s_\nu M M' [(3\bar{g}_A^2 + \bar{g}_V^2) E_e |\mathbf{p}_\nu| \\ & + (\bar{g}_V^2 - \bar{g}_A^2) E_{\nu,s} \mathbf{p}_e \cdot \hat{\mathbf{p}}_\nu] \\ & - g_a a_0 M M' [(3\bar{g}_A^2 + \bar{g}_V^2) E_e \\ & \left. + 2s_\nu (\bar{g}_V^2 - \bar{g}_A^2) \mathbf{p}_e \cdot \hat{\mathbf{p}}_\nu] \right\}. \end{aligned} \quad (C3)$$

With a vanishing a_0 , the result will be reduced to the standard one, which is consistent with Ref. [54]. The matrix element in the vector background has a similar expression, but one can sum over the neutrino helicity, leading to

$$\begin{aligned} \sum_{s,s',s_e,s_\nu} |\mathcal{M}_V|^2 = & 32 G_F^2 |V_{ud}|^2 \left\{ (\bar{g}_V + \bar{g}_A)^2 (p_e \cdot p') \right. \\ & \times (p \cdot \tilde{p}_\nu) + (\bar{g}_V - \bar{g}_A)^2 (p_e \cdot p)(p' \cdot \tilde{p}_\nu) \\ & \left. + (\bar{g}_A^2 - \bar{g}_V^2) M \cdot M' (p_e \cdot \tilde{p}_\nu) \right\}, \end{aligned} \quad (C4)$$

which is close to the standard results but with p_ν in vacuum replaced by $\tilde{p}_\nu = (\tilde{E}_\nu, \mathbf{p}_\nu)$.

The final beta-decay rate without the sum of neutrino helicity reads

$$\Gamma_\beta = \frac{1}{2^9 \pi^5 M} \int \frac{d^3 \mathbf{p}' d^3 \mathbf{p}_e d^3 \mathbf{p}_\nu}{E' E_e \tilde{E}_\nu} \left(\frac{1}{2} \sum_{s,s',s_e} |\mathcal{M}|^2 \right) \times F(Z, E_e) \delta^4(p - p' - p_e - p_\nu). \quad (C5)$$

Note that the neutrino energy in the phase space factor is different from the vacuum case, namely \tilde{E}_ν for the vector background and $\tilde{E} = E_s$ for the axial-vector one, such that the normalization and completeness relations of spinors can appreciate the simple forms as in Eqs. (A5), (A6), (B5) and (B6). In principle, one can take different normalization conventions, but the final result is invariant. The neutrino energy in the delta function should take the form in Eq. (A4) or (B4).

The integration should be done in the rest frame of the tritium, in accordance with the

frame picked out by the dark sea considering the Earth is non-relativistic. After the trivial integration over $d^3\mathbf{p}$ and decomposing $d^3\mathbf{p}_e = |\mathbf{p}_e|^2 d\mathbf{p}_e d\cos\theta_{e\nu} d\phi_{e\nu}$, we have

$$\begin{aligned} \Gamma_\beta = & \frac{1}{2^8 \pi^4 M} \int \frac{|\mathbf{p}_e|^2 d|\mathbf{p}_e| d\cos\theta_{e\nu} d^3\mathbf{p}_\nu}{E' E_e \tilde{E}_\nu} \\ & \times \left(\frac{1}{2} \sum_{s,s',s_e} |\mathcal{M}|^2 \right) F(Z, E_e) \\ & \times \delta(E - E' - E_e - E_\nu). \end{aligned} \quad (\text{C6})$$

Since $d\cos\theta_{e\nu} = E'/(|\mathbf{p}_e| \cdot |\mathbf{p}_\nu|) dE'$ and the neutrino favors no specific direction, the decay rate is simplified to

$$\begin{aligned} \Gamma_\beta = & \frac{1}{2^6 \pi^3 M} \int \frac{dE_e \cdot |\mathbf{p}_\nu| d|\mathbf{p}_\nu|}{\tilde{E}_\nu} \\ & \times \left(\frac{1}{2} \sum_{s,s',s_e} |\mathcal{M}|^2 \right) F(Z, E_e). \end{aligned} \quad (\text{C7})$$

We are left with integrating over the neutrino momentum in order to obtain the differential spectrum with respect to the electron energy. The integration limit can be obtained by requiring that

$$E_\nu(|p_\nu|) + E_e(|p_e|) + E'(|p_\nu|, |p_e|, \cos\theta_{e\nu}) = E,$$

and has a solution of $|p_\nu|$ for any $-1 \leq \cos\theta_{e\nu} \leq 1$ and $m_e \leq E_e \leq E_e^{\max}$. This leads to Eq. (10) for the vector case in the main text. For the axial-vector case, we integrate the rate numerically. It is worthwhile to remark that at the maximal electron energy (i.e., minimal neutrino energy) in the axial-vector case, $|\mathbf{p}| = 2s g_a a_0$, and the phase space factor in Eq. (C7) is not vanishing as in the standard case. This gives rise to a finite decay rate at the endpoint of electron spectrum.

Appendix D: Some remarks on the ground state in the dark sea

The formation of the background field typically takes place on cosmological time scales, say 1 Gyr corresponding to $\sim 1/(2 \times 10^{-32})$ eV, which

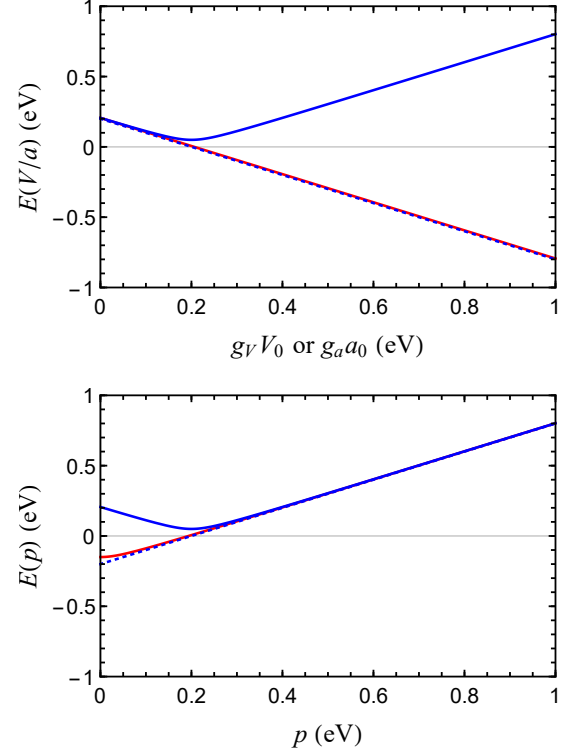


FIG. 3. Upper panel: The evolution of neutrino energy as the dark potential $g_V V_0$ (red curve) or $g_a a_0$ (blue curves) adiabatically increases. The neutrino momentum is taken as $p = 0.2$ eV. Lower panel: The dispersion relation with respect to p with $g_V V_0$ (red curve) or $g_a a_0$ (blue curves) being 0.2 eV. In both panels, for the solid curves the neutrino mass has been set to $m = 0.05$ eV, while for the dotted blue one $m = 0$ eV.

is significantly larger than the Compton frequency of neutrinos, i.e., the inverse of mass $1/m_\nu \approx 6.6 \times 10^{-15}$ s for $m_\nu = 0.1$ eV. The neutrino modes will therefore always stay in their energy eigenstates during the adiabatic formation of the background field, meaning that the eigenvalues of neutrino energy should change in a continuous and smooth manner without transitions.

For the vector and axial-vector cases, let us investigate in more detail how the energy of a neutrino mode evolves when the background field $g_V V_0$ or $g_a a_0$ gradually changes from zero to a certain value. Their dispersion relations for the right-helicity antineutrino (corresponding to

$\overline{\nu_L}$ in the massless limit) are recast as follows:

$$E(V) = \sqrt{p^2 + m^2} - g_V V_0, \quad (\text{D1})$$

$$E(a) = \sqrt{(p - g_a a_0)^2 + m^2}, \quad (\text{D2})$$

where $p \geq 0$ represents the magnitude of neutrino momentum. As long as $m \neq 0$, these are indeed smooth functions of the potential field. To be specific, we take the neutrino mass as $m = 0.05$ eV and set the neutrino momentum to be $p = 0.2$ eV. Then let $g_V V_0$ and $g_a a_0$ adiabatically change from 0 eV to 1 eV. The evolution of energy is shown in upper panel Fig. 3. In the lower panel, we fix $g_V V_0$ and $g_a a_0$ as 0.2 eV and vary p .

For comparison, in both panels of Fig. 3 we give the case of axial-vector potential with vanishing neutrino mass as dotted curves. Special care should be taken when the neutrino mass is vanishing, i.e., $m = 0$ in Eq. (D2). By taking the derivative of Eq. (D2), we have

$$\frac{\partial E}{\partial(g_a a_0)} = -\frac{\partial E}{\partial p} = \frac{g_a a_0 - p}{\sqrt{(p - g_a a_0)^2 + m^2}}. \quad (\text{D3})$$

It is clear that as long as $m \neq 0$, the energy E is a smooth function of a_0 and p . However, when $m = 0$, the derivative becomes ill-defined at $p = g_a a_0$. A smooth solution to the massless case in the axial-vector potential should be

$$E(a) = p - g_a a_0, \quad (\text{D4})$$

which becomes identical to the vector scenario in Eq. (D1). This is exactly what we expect when the neutrino mass is vanishing, for which the difference of results between vector and axial-vector scenarios is supposed to vanish.

The adiabatic evolution of the eigenstates of neutrinos is schematically shown in Fig. 4 for the vector and axial-vector cases, respectively. We explain the figure quantitatively in what follows and note that we have verified it by numerically solving the Dirac equation. For the axial vector case, there is an energy barrier set by the neutrino mass which keeps the neutrino state above the zero-point energy, as $g_a a_0$ adiabatically increases. In the massless limit, such a barrier does not exist, and the left-handed field shifts

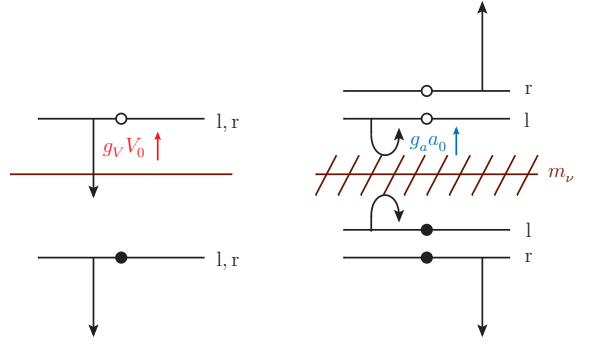


FIG. 4. An illustration of the evolution of the neutrino energy eigenstates, as the magnitude of dark potential $g_V V_0 < 0$ (left panel) or $g_a a_0 < 0$ (right panel) is adiabatically increasing. The baseline of $E_\nu = 0$ is set by the brown line. The state with an empty circle corresponds to the neutrino, while that with a filled circle to the antineutrino. The energy is split for the left-helicity ('l') and right-helicity ('r') states in the axial-vector case. Neutrinos are not allowed to stay in the shaded region on the right.

smoothly down as in the vector case. Because only the left-handed neutrino field is responsible for the beta decays (left-helicity for neutrino and right-helicity for antineutrino in Fig. 4), the effects of axial-vector and vector dark potentials on the beta-decay spectrum should be the same for $m_\nu = 0$.

For the axial-vector potential, the adiabatic approximation will break down in the extremely narrow parameter space $0 < m_\nu \lesssim 10^{-32}$ eV (for which the background field changes faster than the neutrino mass), and one may expect the probability of tunneling crossing the mass barrier (for the massless case without barrier, the tunneling probability is equivalently one). This is very similar to the matter effect of neutrino oscillations in varying matter profile [7]. On the resonance, when the adiabaticity parameter is large $\gamma \gg \mathcal{O}(1)$, the neutrino will always stay in one specific mass eigenstate. But for $\gamma \lesssim \mathcal{O}(1)$, transition occurs from one neutrino mass eigenstate to another.

In Fig. 1 of the main text, in the limit of

$m_\nu \rightarrow 0$, the result of the axial-vector case seems unable to continuously transit to that of the vector one. This is not a surprise considering that the cosmological time scale, one billion years corresponding to 2×10^{-32} eV, separates the massless and sizable massive cases.

Appendix E: Convolution of the response function and fit to KNM1 data

We assume T_2 as the only tritium source, and only the final-state excitations of ${}^3\text{HeT}^+$ need to be considered. Given the accuracy of KATRIN, we use the Gaussian-averaged final-state distributions in Ref. [69]. The response function is dependent on the surplus energy $E_e - qU$, where qU is the applied electric potential. For the fit of the first campaign of KATRIN, we use the response function $f_{\text{res}}(K_e - qU)$ given in Fig. 2 of Ref. [46] for a column density 1.11×10^{17} molecules \cdot cm $^{-2}$. The ring-averaged event rate as in Fig. 3 of Ref. [46] will be used as the input of experimental measurements. The key of the fit is to compare the observed event rate with the theory prediction

$$R_{\text{th}} = A_s N_T \int f_{\text{res}}(K_e - qU) \frac{d\Gamma_\beta}{dK_e} dK_e + R_{\text{bkg}},$$

where A_s is the normalization factor, N_T is the total tritium number, qU is the applied retarding potential, and R_{bkg} is the background rate. The variables A_s , R_{bkg} and m_ν^2 are taken as free parameters.

For the present KATRIN sensitivity, the major effects of the vector and axial-vector potentials are to shift the endpoint energy E_0 of electrons. Hence their effects are entirely ascribed to the fit of E_0 at KATRIN. For this purpose, we vary freely the vacuum neutrino mass over $m_\nu^2 \geq 0$. In the official fit of KATRIN, the $m_\nu^2 < 0$ region is kept to account for data fluctuations, but eventually it is removed by proper statistical interpretations in obtaining the mass limit. We adopt here a simplified approach with the main interest being the minimized χ^2 , whose function for KNM1 is constructed as

$$\chi_\beta^2(m_\nu^2, E_0, A_s, R_{\text{bkg}}) = \left(\frac{R_{\text{th}}^i - R_{\text{exp}}^i}{\sigma_{\text{exp}}^i} \right)^2, \quad (\text{E1})$$

where the uncertainty σ_{exp}^i is taken from Fig. 3 of Ref. [46] for each retarding potential qU_i . Note that only the dominant statistical error is taken into account. The effects of scalar and pseudoscalar potentials are indistinguishable from neutrino mass. We hence assume the vacuum neutrino mass to be vanishing and vary other parameters E_0 , A_s and R_{bkg} freely.

We do not attempt to fit the KNM2 results here, for which the statistical framework should account for every detector ring and there is not sufficient information to perform the fit ourselves. As has been mentioned in the main text, for KNM2 we take the existing results $m_\nu^2 = 0.26 \pm 0.34$ eV 2 and $E_0 = 18573.69 \pm 0.03$ eV as our direct inputs with approximations. In this case, only a small part of the $m_\nu^2 < 0$ region is included in the χ^2 minimization procedure, which should be tolerable.

[1] L. Wolfenstein, “*Neutrino Oscillations in Matter*,” *Phys. Rev. D* **17** (1978) 2369–2374.

[2] L. Wolfenstein, “*Neutrino Oscillations and Stellar Collapse*,” *Phys. Rev. D* **20** (1979) 2634–2635.

[3] S. P. Mikheyev and A. Y. Smirnov, “*Resonance Amplification of Oscillations in Matter and Spectroscopy of Solar Neutrinos*,” Sov. J. Nucl. Phys. **42** (1985) 913–917.

[4] S. P. Mikheyev and A. Y. Smirnov, “*Resonant amplification of neutrino oscillations in matter and solar neutrino spectroscopy*,” *Nuovo Cim. C* **9** (1986) 17–26.

[5] A. Halprin, “*Neutrino Oscillations in Nonuniform Matter*,” *Phys. Rev. D* **34** (1986) 3462–3466.

- [6] L. N. Chang and R. K. P. Zia, “*Anomalous Propagation of Neutrino Beams Through Dense Media*,” *Phys. Rev. D* **38** (1988) 1669.
- [7] T.-K. Kuo and J. T. Pantaleone, “*Neutrino Oscillations in Matter*,” *Rev. Mod. Phys.* **61** (1989) 937.
- [8] R. F. Sawyer, “*Neutrino oscillations in inhomogeneous matter*,” *Phys. Rev. D* **42** (1990) 3908–3917.
- [9] G. G. Raffelt, *Stars as laboratories for fundamental physics: The astrophysics of neutrinos, axions, and other weakly interacting particles*. 5, 1996.
- [10] C. Y. Cardall and D. J. H. Chung, “*The MSW effect in quantum field theory*,” *Phys. Rev. D* **60** (1999) 073012, [arXiv:hep-ph/9904291](https://arxiv.org/abs/hep-ph/9904291).
- [11] K. Fujii, C. Habe, and M. Blasone, “*Operator relation among neutrino fields and oscillation formulas in matter*,” [arXiv:hep-ph/0212076](https://arxiv.org/abs/hep-ph/0212076).
- [12] J. Linder, “*Derivation of neutrino matter potentials induced by earth*,” [arXiv:hep-ph/0504264](https://arxiv.org/abs/hep-ph/0504264).
- [13] E. K. Akhmedov and A. Wilhelm, “*Quantum field theoretic approach to neutrino oscillations in matter*,” *JHEP* **01** (2013) 165, [arXiv:1205.6231](https://arxiv.org/abs/1205.6231).
- [14] M. Blennow and A. Y. Smirnov, “*Neutrino propagation in matter*,” *Adv. High Energy Phys.* **2013** (2013) 972485, [arXiv:1306.2903](https://arxiv.org/abs/1306.2903).
- [15] E. Akhmedov, “*Neutrino oscillations in matter: from microscopic to macroscopic description*,” *JHEP* **02** (2021) 107, [arXiv:2010.07847](https://arxiv.org/abs/2010.07847).
- [16] A. Berlin, “*Neutrino Oscillations as a Probe of Light Scalar Dark Matter*,” *Phys. Rev. Lett.* **117** (2016) no. 23, 231801, [arXiv:1608.01307](https://arxiv.org/abs/1608.01307).
- [17] V. Brdar, J. Kopp, J. Liu, P. Prass, and X.-P. Wang, “*Fuzzy dark matter and nonstandard neutrino interactions*,” *Phys. Rev. D* **97** (2018) no. 4, 043001, [arXiv:1705.09455](https://arxiv.org/abs/1705.09455).
- [18] G. Krnjaic, P. A. N. Machado, and L. Necib, “*Distorted neutrino oscillations from time varying cosmic fields*,” *Phys. Rev. D* **97** (2018) no. 7, 075017, [arXiv:1705.06740](https://arxiv.org/abs/1705.06740).
- [19] J. Liao, D. Marfatia, and K. Whisnant, “*Light scalar dark matter at neutrino oscillation experiments*,” *JHEP* **04** (2018) 136, [arXiv:1803.01773](https://arxiv.org/abs/1803.01773).
- [20] F. Capozzi, I. M. Shoemaker, and L. Vecchi, “*Neutrino Oscillations in Dark Backgrounds*,” *JCAP* **07** (2018) 004, [arXiv:1804.05117](https://arxiv.org/abs/1804.05117).
- [21] M. M. Reynoso and O. A. Sampayo, “*Propagation of high-energy neutrinos in a background of ultralight scalar dark matter*,” *Astropart. Phys.* **82** (2016) 10–20, [arXiv:1605.09671](https://arxiv.org/abs/1605.09671).
- [22] G.-Y. Huang and N. Nath, “*Neutrinophilic Axion-Like Dark Matter*,” *Eur. Phys. J. C* **78** (2018) no. 11, 922, [arXiv:1809.01111](https://arxiv.org/abs/1809.01111).
- [23] S. Pandey, S. Karmakar, and S. Rakshit, “*Interactions of Astrophysical Neutrinos with Dark Matter: A model building perspective*,” *JHEP* **01** (2019) 095, [arXiv:1810.04203](https://arxiv.org/abs/1810.04203).
- [24] Y. Farzan and S. Palomares-Ruiz, “*Flavor of cosmic neutrinos preserved by ultralight dark matter*,” *Phys. Rev. D* **99** (2019) no. 5, 051702, [arXiv:1810.00892](https://arxiv.org/abs/1810.00892).
- [25] K.-Y. Choi, J. Kim, and C. Rott, “*Constraining dark matter-neutrino interactions with IceCube-170922A*,” *Phys. Rev. D* **99** (2019) no. 8, 083018, [arXiv:1903.03302](https://arxiv.org/abs/1903.03302).
- [26] S. Baek, “*Dirac neutrino from the breaking of Peccei-Quinn symmetry*,” *Phys. Lett. B* **805** (2020) 135415, [arXiv:1911.04210](https://arxiv.org/abs/1911.04210).
- [27] K.-Y. Choi, E. J. Chun, and J. Kim, “*Neutrino Oscillations in Dark Matter*,” *Phys. Dark Univ.* **30** (2020) 100606, [arXiv:1909.10478](https://arxiv.org/abs/1909.10478).
- [28] K.-Y. Choi, E. J. Chun, and J. Kim, “*Dispersion of neutrinos in a medium*,” [arXiv:2012.09474](https://arxiv.org/abs/2012.09474).
- [29] A. Dev, P. A. N. Machado, and P. Martínez-Miravé, “*Signatures of ultralight dark matter in neutrino oscillation experiments*,” *JHEP* **01** (2021) 094, [arXiv:2007.03590](https://arxiv.org/abs/2007.03590).
- [30] S. Baek, “*A connection between flavour anomaly, neutrino mass, and axion*,” *JHEP* **10** (2020) 111, [arXiv:2006.02050](https://arxiv.org/abs/2006.02050).

- [31] M. Losada, Y. Nir, G. Perez, and Y. Shpilman, “*Probing scalar dark matter oscillations with neutrino oscillations*,” [arXiv:2107.10865](https://arxiv.org/abs/2107.10865).
- [32] A. Y. Smirnov and V. B. Valera, “*Resonance refraction and neutrino oscillations*,” [arXiv:2106.13829](https://arxiv.org/abs/2106.13829).
- [33] G. Alonso-Álvarez and J. M. Cline, “*Sterile neutrino dark matter catalyzed by a very light dark photon*,” [arXiv:2107.07524](https://arxiv.org/abs/2107.07524).
- [34] S.-F. Ge and H. Murayama, “*Apparent CPT Violation in Neutrino Oscillation from Dark Non-Standard Interactions*,” [arXiv:1904.02518](https://arxiv.org/abs/1904.02518).
- [35] H. Davoudiasl, G. Mohlabeng, and M. Sullivan, “*Galactic Dark Matter Population as the Source of Neutrino Masses*,” *Phys. Rev. D* **98** (2018) no. 2, 021301, [arXiv:1803.00012](https://arxiv.org/abs/1803.00012).
- [36] A. S. Joshipura and S. Mohanty, “*Constraints on flavor dependent long range forces from atmospheric neutrino observations at super-Kamiokande*,” *Phys. Lett. B* **584** (2004) 103–108, [arXiv:hep-ph/0310210](https://arxiv.org/abs/hep-ph/0310210).
- [37] J. A. Grifols and E. Masso, “*Neutrino oscillations in the sun probe long range leptonic forces*,” *Phys. Lett. B* **579** (2004) 123–126, [arXiv:hep-ph/0311141](https://arxiv.org/abs/hep-ph/0311141).
- [38] A. Bandyopadhyay, A. Dighe, and A. S. Joshipura, “*Constraints on flavor-dependent long range forces from solar neutrinos and KamLAND*,” *Phys. Rev. D* **75** (2007) 093005, [arXiv:hep-ph/0610263](https://arxiv.org/abs/hep-ph/0610263).
- [39] J. Heeck and W. Rodejohann, “*Gauged $L_\mu - L_\tau$ and different Muon Neutrino and Anti-Neutrino Oscillations: MINOS and beyond*,” *J. Phys. G* **38** (2011) 085005, [arXiv:1007.2655](https://arxiv.org/abs/1007.2655).
- [40] M. B. Wise and Y. Zhang, “*Lepton Flavorful Fifth Force and Depth-dependent Neutrino Matter Interactions*,” *JHEP* **06** (2018) 053, [arXiv:1803.00591](https://arxiv.org/abs/1803.00591).
- [41] S.-F. Ge and S. J. Parke, “*Scalar Nonstandard Interactions in Neutrino Oscillation*,” *Phys. Rev. Lett.* **122** (2019) no. 21, 211801, [arXiv:1812.08376](https://arxiv.org/abs/1812.08376).
- [42] A. Y. Smirnov and X.-J. Xu, “*Wolfenstein potentials for neutrinos induced by ultra-light mediators*,” *JHEP* **12** (2019) 046, [arXiv:1909.07505](https://arxiv.org/abs/1909.07505).
- [43] K. S. Babu, G. Chauhan, and P. S. Bhupal Dev, “*Neutrino nonstandard interactions via light scalars in the Earth, Sun, supernovae, and the early Universe*,” *Phys. Rev. D* **101** (2020) no. 9, 095029, [arXiv:1912.13488](https://arxiv.org/abs/1912.13488).
- [44] M. Bustamante and S. K. Agarwalla, “*Universe’s Worth of Electrons to Probe Long-Range Interactions of High-Energy Astrophysical Neutrinos*,” *Phys. Rev. Lett.* **122** (2019) no. 6, 061103, [arXiv:1808.02042](https://arxiv.org/abs/1808.02042).
- [45] P. Coloma, M. C. Gonzalez-Garcia, and M. Maltoni, “*Neutrino oscillation constraints on $U(1)'$ models: from non-standard interactions to long-range forces*,” *JHEP* **01** (2021) 114, [arXiv:2009.14220](https://arxiv.org/abs/2009.14220).
- [46] **KATRIN**, M. Aker *et al.*, “*Improved Upper Limit on the Neutrino Mass from a Direct Kinematic Method by KATRIN*,” *Phys. Rev. Lett.* **123** (2019) no. 22, 221802, [arXiv:1909.06048](https://arxiv.org/abs/1909.06048).
- [47] **KATRIN**, M. Aker *et al.*, “*Analysis methods for the first KATRIN neutrino-mass measurement*,” *Phys. Rev. D* **104** (2021) no. 1, 012005, [arXiv:2101.05253](https://arxiv.org/abs/2101.05253).
- [48] M. Aker *et al.*, “*First direct neutrino-mass measurement with sub-eV sensitivity*,” [arXiv:2105.08533](https://arxiv.org/abs/2105.08533).
- [49] S. P. Rosen, “*Analog of the Michel Parameter for Neutrino - Electron Scattering: A Test for Majorana Neutrinos*,” *Phys. Rev. Lett.* **48** (1982) 842.
- [50] W. Rodejohann, X.-J. Xu, and C. E. Yaguna, “*Distinguishing between Dirac and Majorana neutrinos in the presence of general interactions*,” *JHEP* **05** (2017) 024, [arXiv:1702.05721](https://arxiv.org/abs/1702.05721).
- [51] R. E. Shrock, “*New Tests For, and Bounds On, Neutrino Masses and Lepton Mixing*,” *Phys. Lett.* **96B** (1980) 159–164.
- [52] S. S. Masood, S. Nasri, J. Schechter, M. A. Tortola, J. W. F. Valle, and C. Weinheimer,

“Exact relativistic beta decay endpoint spectrum,” *Phys. Rev. C* **76** (2007) 045501, [arXiv:0706.0897](https://arxiv.org/abs/0706.0897).

[53] F. Simkovic, R. Dvornicky, and A. Faessler, “Exact relativistic tritium beta-decay endpoint spectrum in a hadron model,” *Phys. Rev. C* **77** (2008) 055502, [arXiv:0712.3926](https://arxiv.org/abs/0712.3926).

[54] A. J. Long, C. Lunardini, and E. Sabancilar, “Detecting non-relativistic cosmic neutrinos by capture on tritium: phenomenology and physics potential,” *JCAP* **1408** (2014) 038, [arXiv:1405.7654](https://arxiv.org/abs/1405.7654).

[55] P. O. Ludl and W. Rodejohann, “Direct Neutrino Mass Experiments and Exotic Charged Current Interactions,” *JHEP* **06** (2016) 040, [arXiv:1603.08690](https://arxiv.org/abs/1603.08690).

[56] **Planck**, N. Aghanim *et al.*, “Planck 2018 results. VI. Cosmological parameters,” *Astron. Astrophys.* **641** (2020) A6, [arXiv:1807.06209](https://arxiv.org/abs/1807.06209). [Erratum: *Astron. Astrophys.* 652, C4 (2021)].

[57] L. Gastaldo *et al.*, “The electron capture in ^{163}Ho experiment – ECHO,” *Eur. Phys. J. ST* **226** (2017) no. 8, 1623–1694.

[58] **KATRIN**, J. Angrik *et al.*, “KATRIN design report 2004.”

[59] L. G. van den Aarssen, T. Bringmann, and C. Pfrommer, “Is dark matter with long-range interactions a solution to all small-scale problems of Λ CDM cosmology?,” *Phys. Rev. Lett.* **109** (2012) 231301, [arXiv:1205.5809](https://arxiv.org/abs/1205.5809).

[60] H. Ruegg and M. Ruiz-Altaba, “The Stueckelberg field,” *Int. J. Mod. Phys. A* **19** (2004) 3265–3348, [arXiv:hep-th/0304245](https://arxiv.org/abs/hep-th/0304245).

[61] S. Schlamminger, K. Y. Choi, T. A. Wagner, J. H. Gundlach, and E. G. Adelberger, “Test of the equivalence principle using a rotating torsion balance,” *Phys. Rev. Lett.* **100** (2008) 041101, [arXiv:0712.0607](https://arxiv.org/abs/0712.0607).

[62] A. D. Dolgov and G. G. Raffelt, “Screening of long range leptonic forces by cosmic background neutrinos,” *Phys. Rev. D* **52** (1995) 2581–2582, [arXiv:hep-ph/9503438](https://arxiv.org/abs/hep-ph/9503438).

[63] L. Ackerman, M. R. Buckley, S. M. Carroll, and M. Kamionkowski, “Dark Matter and Dark Radiation,” *Phys. Rev. D* **79** (2009) 023519, [arXiv:0810.5126](https://arxiv.org/abs/0810.5126).

[64] P. Agrawal, F.-Y. Cyr-Racine, L. Randall, and J. Scholtz, “Make Dark Matter Charged Again,” *JCAP* **05** (2017) 022, [arXiv:1610.04611](https://arxiv.org/abs/1610.04611).

[65] R. Lasenby, “Long range dark matter self-interactions and plasma instabilities,” *JCAP* **11** (2020) 034, [arXiv:2007.00667](https://arxiv.org/abs/2007.00667).

[66] M. Kesden and M. Kamionkowski, “Tidal Tails Test the Equivalence Principle in the Dark Sector,” *Phys. Rev. D* **74** (2006) 083007, [arXiv:astro-ph/0608095](https://arxiv.org/abs/astro-ph/0608095).

[67] M. Kesden and M. Kamionkowski, “Galilean Equivalence for Galactic Dark Matter,” *Phys. Rev. Lett.* **97** (2006) 131303, [arXiv:astro-ph/0606566](https://arxiv.org/abs/astro-ph/0606566).

[68] S. M. Carroll, S. Mantry, M. J. Ramsey-Musolf, and C. W. Stubbs, “Dark-Matter-Induced Weak Equivalence Principle Violation,” *Phys. Rev. Lett.* **103** (2009) 011301, [arXiv:0807.4363](https://arxiv.org/abs/0807.4363).

[69] N. Doss, J. Tennyson, A. Saenz, and S. Jonsell, “Molecular effects in investigations of tritium molecule beta decay endpoint experiments,” *Phys. Rev. C* **73** (2006) 025502.